Organic & Biomolecular Chemistry

ROYAL SOCIETY OF CHEMISTRY

COMMUNICATION

View Article Online
View Journal | View Issue

Open Access Article. Published on 12 jlijs 2021. Downloaded on 24.02.2026 07:36:42.
This article is licensed under a Creative Commons Attribution-NonCommercial 3.0 Unported Licence.

Cite this: *Org. Biomol. Chem.*, 2021, **19**, 6633

Received 19th June 2021,
Accepted 7th July 2021

DOI: 10.1039/d1ob01185e

rsc.li/obc

Comparison of $[Pd_2L_4][BF_4]_4$ cages for binding of *n*-octyl glycosides and nitrate (L = isophthalamide or dipicolinamide linked dipyridyl ligand)†

Brian J. J. Timmer, Eduard O. Bobylev and Tiddo J. Mooibroek *

Two dipyridyl ligands were synthesized, where the pyridyl donor fragments were separated by an isophthalamide (1) or a dipicolinamide moiety (2). Both ligands formed $[Pd_2(Ligand)_4][BF_4]_4$ complexes in CD_2Cl_2 containing 5% dmso-d_6. It was found that while $[Pd_2(1)_4][BF_4]_4$ readily binds to *n*-octyl glycosides and to nitrate anions, $[Pd_2(2)_4][BF_4]_4$ did not. The difference in binding properties could be rationalized based on the reduced flexibility and size of the $[Pd_2(2)_4]^{2+}$ cage and/or stronger interior binding of a BF_4^- counter anion.

Introduction

It is well-known that cage complexes of the type $[M_2L_4]^{4+}$ are readily prepared when the metal (M) is a divalent Pd^{2+} ion and the ligand (L) is a dipyridyl ligand.[1] Such complexes typically exhibit a hollow interior that is suitable to host smaller molecules.[1a,2] Recently, it was shown that such $[M_2L_4]^{4+}$ complexes could be used to bind carbohydrates.[3] In particular, it was shown that a dipyridyl ligand such as **1** in Fig. 1 formed a $[Pd_2L_4]^{2+}$ cage[4] that could bind to *n*-octyl-β-D-glucoside.[3c] As is highlighted in red in Fig. 1, the amides in a cage derived from **1** experience a steric clash with the isophthalamide's central C–H fragment. We wondered what the effect would be of C–H → N adjustment of **1** to the dipicolinamide analogue **2**, where the amides should be preorganized by intramolecular N–H···N hydrogen bonds (also highlighted in red).[5] Herein, we report on the synthesis of **1** and **2** and their $[Pd_2(Ligand)_4][BF_4]_4$ complexes and shown that the C–H → N adjustment is detrimental to the binding properties of the cage.

Van 't Hoff Institute for Molecular Sciences, University of Amsterdam, Science Park 904, 1098 XH Amsterdam, The Netherlands. E-mail: t.j.mooibroek@uva.nl

†Electronic supplementary information (ESI) available. See DOI: 10.1039/d1ob01185e

Results and discussion

As is detailed in the ESI (section S2†), ligands **1** and **2** could easily be prepared according to known chemistry adapted from literature procedures.[3c,6] Instead of the –C(O)NHCH$_2$C((CH$_2$)$_2$*t*-Bu)$_3$ solubilizing group used in a previous version of **1**,[3c] we opted for the –(CH$_2$)$_2$O-*p*-Ph-C(*p*-*t*Bu-Ph)$_3$ group[6a] due to the more facile synthesis, particularly to obtain the dipicolinamide derived ligand. Stepwise addition of 0.5 equivalents of $[Pd(OSMe_2)_4][BAr^F]_2$ to a solution of **1** in CD_2Cl_2 containing 5% dmso-d_6 led to the formation of single species on NMR, most likely $[Pd_2\mathbf{1}_4][BAr^F]_4$ (Fig. S32,† BAr^F = tetrakis[3,5-bis(trifluoromethyl)phenyl]borate). Following the same procedure with ligand **2** however, gave complicated spectra that did not resolve to a neat spectrum, not even after standing for a week (Fig. S33†). Repeating the procedure but with $[Pd(NCMe)_4][BF_4]_2$ gave clearly resolved spectra for both **1** and **2** after standing for 7 days and these final spectra are shown in Fig. 2. The difference in complex formation is likely due to a templating effect of BF_4^-.[7] For the dipyridyl ligand **1** (Fig. 2a), the inwards facing **s3NH**, **p2** and **s4** displayed significant downfield shifts that are characteristic of $[Pd_2(Ligand)_4]^{4+}$ formation.[3c,d] With ligand **2** (Fig. 2b) the inwards facing **s3NH** and **p2** underwent an upfield shift upon Pd-coordination. With both ligands, the resonances belonging to the CH's of the solubilizing groups remained unperturbed. Moreover, DOSY-NMR showed that the complexes had a larger diffusion constant than their parent ligand, which is consistent with formation of $[Pd_2(Ligand)_4]^{2+}$ complexes. A thorough NMR spectroscopic evaluation of the complexes was also consistent with the formation of $[Pd_2\mathbf{1}_4]^{4+}$ and $[Pd_2\mathbf{2}_4]^{4+}$ and high resolution mass spectroscopy of both complexes was congruent with the 2 : 4 molar ratio of Pd to ligand (see Fig. S23 and S32†).

The binding affinities of both complexes for carbohydrates **3–6** listed in Table 1 was probed by ^{1}H-NMR titration experiments in CD_2Cl_2 containing 5% dmso-d_6.

As is illustrated in Fig. 3 for the titrations with *n*-octyl-β-D-mannoside **3**, significant peak shifting was observed for

Open Access Article. Published on 12 jlijs 2021. Downloaded on 24.02.2026 07:36:42.
This article is licensed under a Creative Commons Attribution-NonCommercial 3.0 Unported Licence.

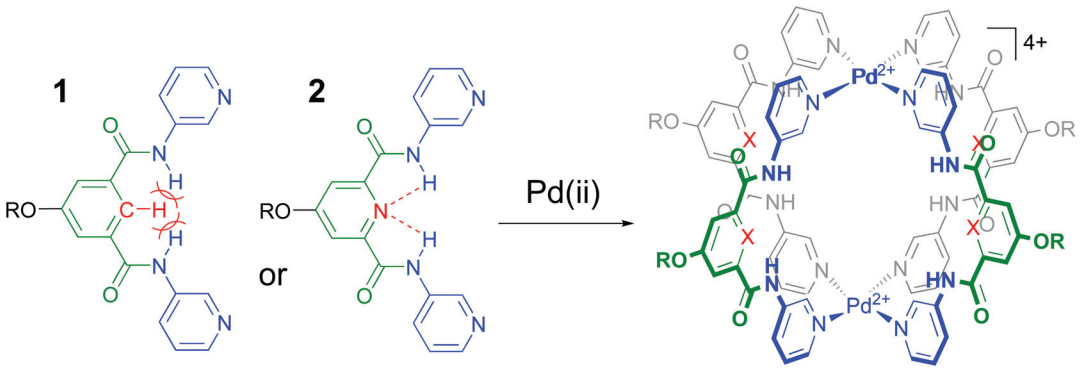

Fig. 1 Ligands **1** and **2** used in this study to make $[Pd_2(Ligand)_4]^{4+}$ complexes. R = solubility group = $-(CH_2)_2O$-*p*-Ph-C(*p*-*t*Bu-Ph)$_3$. See section S2† for synthetic details and see Fig. S52† for a model of the steric clash present in **1**.

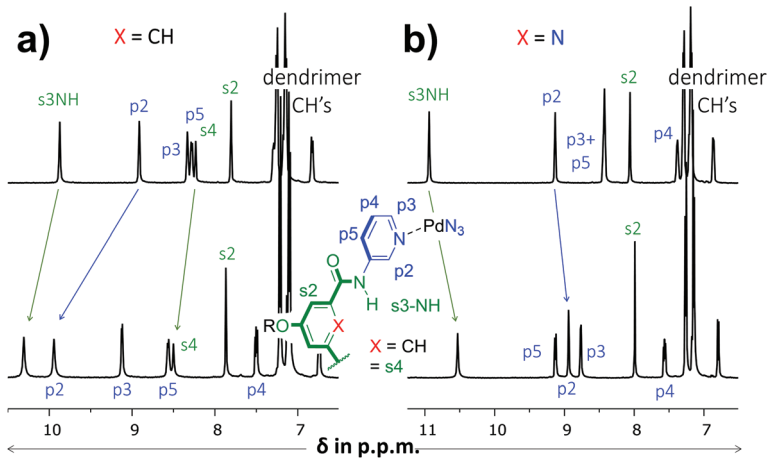

Fig. 2 Partial ^{1}H NMR spectra involving dipyridyl ligands **1** (a) and **2** (b). The top spectra are of pure ligand and the bottom spectra are of the $[Pd_2(Ligand)_4[BF_4]_4$ complexes. The solvent is CD_2Cl_2 containing 5% dmso-d_6 and further details are given in the ESI.†

$[Pd_2\mathbf{1}_4]^{4+}$ (Fig. 3a) in the concentration range to 25 mM of **3**. Shifting of peaks cannot result from the dilution of the complex, as dilution studies in the concentration range used during titrations (0.64–0.27 mM) revealed that all resonances remained stationary (see Fig. S36†). The resonances that shift most are the inwards pointing **s3NH**, **p2** and **s4**. The peak shifts could be analyzed using HypNMR, as is shown in the left-hand side of Fig. 3a. From this plot it is evident that all resonances display clear saturation behavior around 10 mM of **3**. Fitting these shifts with HypNMR[8] to a 1 : 1 binding model gave K_a = 541 ± 2.9 M^{-1} with a reasonable accuracy (r^2 = 0.9862). Similar spectra and fits were obtained by titrations of $[Pd_2\mathbf{1}_4]^{4+}$ with the other carbohydrates. Moreover, NOESY spectroscopy of solutions of $[Pd_2\mathbf{1}_4]^{4+}$ containing galactoside **3** or glucoside **5** were consistent with carbohydrate binding to the interior of the cage (see Fig. S43 and S47†). Mass spectroscopic analysis of a solution of $[Pd_2\mathbf{1}_4]^{4+}$ with glucoside **5** supports a 1 : 1 binding stoichiometry (see Fig. S44†).

In sharp contrast to the titrations with $[Pd_2\mathbf{1}_4]^{4+}$, the spectrum of $[Pd_2\mathbf{2}_4]^{4+}$ (Fig. 3b) remained unperturbed when adding **3** to a concentration of 25 mM. Particularly surprising was the complete absence of any shifting of the inwards facing **p2**, which is very characteristic for binding to the interior of these type of M_2L_4 cages.[3c,d] Very similar titration data could be collected with carbohydrates **4**–**6** (see Table 1).

The twofold selectivity of $[Pd_2\mathbf{1}_4]^{4+}$ for β-glucoside **5** over β-galactoside **6** is consistent with an earlier report of the same cage with an alternative solubilizing group (measured in 10% dmso-d_6 in CD_2Cl_2).[3c] Surprisingly, the cage binds strongest to α-mannoside **3** (K_a = 541 M^{-1}), while the affinity for α-glucoside **4** is the same as that measured for β-galactoside **6** (K_a = 261 M^{-1}). These data thus shown that $[Pd_2\mathbf{1}_4]^{4+}$ binds well with all carbohydrates in the order **3** > **5** > **4** = **6**.

Another noticeable observation from Table 1 is the lack of binding of $[Pd_2\mathbf{2}_4]^{4+}$ for all four carbohydrates. This made us wonder if the interior of $[Pd_2\mathbf{2}_4]^{4+}$ was capable of binding at all. To this end, a titration was conducted with $(n\text{-Bu})_4N^+NO_3^-$. As is shown in Fig. 4, very significant peak shifting was observed which appear to saturate around 13 mM of NO_3^-.

Interestingly, while **s3NH** and **p2** only shifted downfield, the resonance of **p3** initially shifted upfield, but then downfield. Such behavior is evidence of a binding stoichiometry

 This journal is © The Royal Society of Chemistry 2021

Open Access Article. Published on 12 jilijs 2021. Downloaded on 24.02.2026 07:36:42.
This article is licensed under a Creative Commons Attribution-NonCommercial 3.0 Unported Licence.

Table 1 Overview of binding studies performed using *n*-octyl-glycosides **3**–**6** (with axial groups highlighted in blue) and NO_3^- in CD_2Cl_2 containing 5% dmso-d_6

	K_a of 1 : 1 binding[a] (M^{-1})	
Host → Guest ↓	$[Pd_2\mathbf{1}_4]^{4+}$	$[Pd_2\mathbf{2}_4]^{4+}$
3	541	i.p.s.[b]
4	262	
5	447	
6	262	
NO_3^-	1862[c]	159[c]

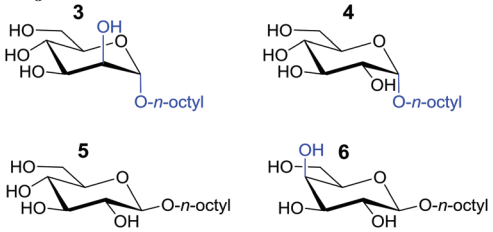

[a] Binding constants were obtained by fitting observed chemical shift differences with HypNMR[8] as is detailed in section S3 of the ESI.† [b] 'i.p.s.' stands for the relatively 'insignificant peak-shifts' that were observed in the concentration range of 0–25 mM glycoside. [c] Incorporating the higher concentration ranges, the affinities could only be modelled with a more complicated stoichiometry than simple 1 : 1 binding, but the 1 : 1 stoichiometries were still dominant or representative of the binding strength of the cages for nitrate anions. Details are provided in the text and in Fig. S42† for $[Pd_2\mathbf{1}_4]^{4+}$ and Fig. S48† for $[Pd_2\mathbf{2}_4]^{4+}$.

that is more complex than simple 1 : 1 binding. As is detailed in the ESI (Fig. S52†), these shifts could be modelled to a 1 : 3 binding model with a $K_a^{1:1}$ = 159, $K_a^{1:2}$ = 63 M^{-1} and $K_a^{1:3}$ = 31 M^{-1} (r^2 = 0.9968). Such a stoichiometry is consistent with a nitrate anion binding to the interior of $[Pd_2\mathbf{2}_4]^{4+}$ (**s3NH** and **p2** shifts) as well as with both exterior sites involving **p3**, in close proximity to both $[Pd(pyridyl)_4]^{2+}$ environments. It has indeed been noted that such a binding mode, involving four charge assisted $[C–H]^+\cdots$nitrate interaction, is common in $[Pd(pyridyl)_4]^{2+}$ complexes.[5b,9] The order of magnitude of nitrate binding of $[Pd_2\mathbf{2}_4]^{4+}$ can be seen as weak, as (in the same matrix) a comparable $[Pd(pyridyl)_4]^{2+}$ complex has been reported with $K_a^{1:1}$ = 91 960 M^{-1}.[9a] A very similar titration involving $[Pd_2\mathbf{1}_4]^{4+}$ could also be modelled with this 1 : 3 stoichiometry (Fig. S46†), but in this instance with a $K_a^{1:1}$ = 1864 M^{-1} (and smaller $K_a^{1:2}$ = 537 M^{-1} and $K_a^{1:3}$ = 316 M^{-1}, with r^2 = 0.957).

It thus appears that $[Pd_2\mathbf{1}_4]^{4+}$ readily hosts other molecules, but its CH → N analogue does not. To gain insight into the possible origin for this loss in binding capability, molecular modeling was conducted using density functional theory (DFT). The resulting models are shown in space filling mode in the left-hand side of Fig. 5 and are similar to previously reported crystal structures (see also Fig. S54 and S55†).[4b,5b] Also given in the figure are the inner dimensions (in Å) of the

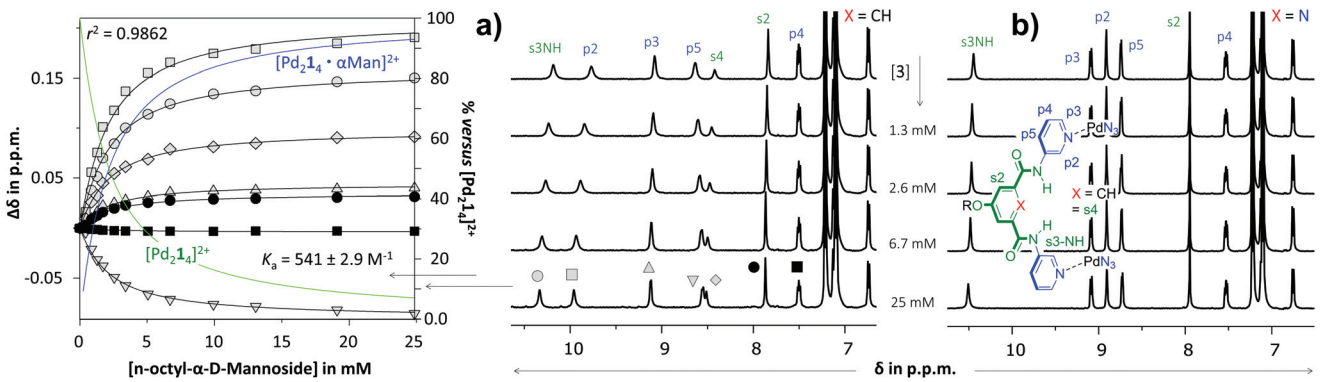

Fig. 3 Partial ^{1}H NMR spectra of titration experiments with *n*-octyl-β-D-mannoside **3** added to a solution of $[Pd_2\mathbf{1}_4][BF_4]_4$ (a) or $[Pd_2\mathbf{2}_4][BF_4]_4$ (b). The peak shifting observed in the titration with $[Pd_2\mathbf{1}_4][BF_4]_4$ were fitted with HypNMR[8] as shown in the left. The solvent is CD_2Cl_2 containing 5% dmso-d_6. Further details are provided in section S40 of the ESI.†

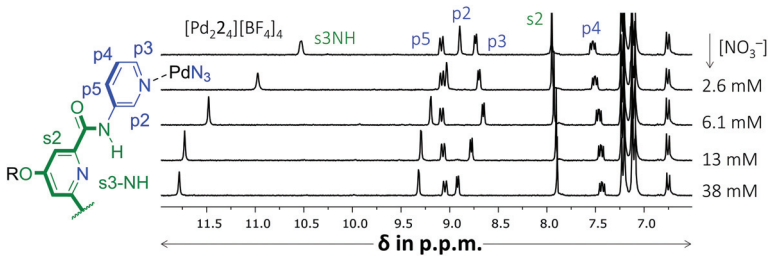

Fig. 4 Partial ^{1}H NMR spectra of a binding study with $(n\text{-Bu})_4N^+NO_3^-$ added to $[Pd_2\mathbf{2}_4][BF_4]_4$. The solvent is CD_2Cl_2 containing 5% dmso-d_6. See Fig. S52† for details.

Open Access Article. Published on 12 jilijs 2021. Downloaded on 24.02.2026 07:36:42.
This article is licensed under a Creative Commons Attribution-NonCommercial 3.0 Unported Licence.

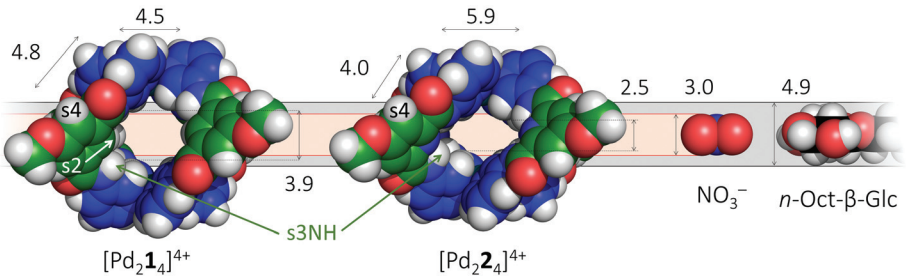

Fig. 5 Space filling representations of molecular models of both $[Pd_2(Ligand)_4]^{4+}$ complexes as well as a nitrate anion and the sugar part of *n*-octyl-β-D-glucoside **5**. The van der Waals corrected dimensions of the interior of the complexes and the exterior of NO_3^- and the glucoside are given in Å. Models generated with DFT/ωB97X-D/6-31G*.

models that were obtained by measuring intramolecular distances and subtracting twice the van der Waals radius of Hydrogen (1.09 Å) or Nitrogen (1.55 Å). While the complex with ligand **2** is about 1.4 Å wider (N–N *versus* CH–HC distance), the complex is also 1.4 Å less high (2.5 *versus* 3.9 Å). Actually, the height of $[Pd_2\mathbf{2}_4]^{4+}$ of 2.5 Å is just large enough for host a nitrate anion (3.0 Å in height) when assuming van der Waals overlap in the order of 0.5 Å. However, the 2.5 Å height of $[Pd_2\mathbf{2}_4]^{4+}$ is much smaller than the height of a glucoside (4.9 Å) and as a result very unlikely to fit. The dimensions of $[Pd_2\mathbf{1}_4]^{4+}$ on the other hand are much more congruent with the dimensions of NO_3^- and a glucoside, thus rationalizing why this complex binds to both (and with much greater affinities). Moreover, due to the preorganization of the amides in ligand **2** (see Fig. 1) its complex is expected to be very rigid. As a result, $[Pd_2\mathbf{2}_4]^{4+}$ might well lack the conformational flexibility that could enable it to encapsulate a glycoside. Such a rational was also proposed previously for the comparison of isophthalamide *versus* dipicolinamide covalent cages in carbohydrate binding.[10] Actually, inspection of the NOESY spectrum of $[Pd_2\mathbf{2}_4]^{4+}$ (Fig. S27†) reveals the complete absence of a close proximity of the amide hydrogens (**s3NH**) and the aromatic **CH** hydrogens (**s2**) of the dipicolinamide fragment. This indeed implies that rotation of the amides is locked into a position with the NH hydrogens pointing to the interior of the complex (bound by the dipicolinic N). In the NOESY spectrum of $[Pd_2\mathbf{1}_4]^{4+}$ (Fig. S20†) on the other hand there is a clear nuclear Overhauser effect cross peak between the amidic NH's and the inwards pointing **s4**, as well as the outwards pointing **s2**. This is consistent with the reported flexibility of these amides in the solid state structures of related cage complexes.[4] Finally, modelling of interior bound BF_4^- (Fig. S55†) shows a much tighter and energetically more stable fit within the $[Pd_2\mathbf{2}_4]^{4+}$ binding pocket, suggesting that interior bound BF_4^- might hamper further binding. Such an adverse effect of BF_4^- on the binding potential of an M_2L_4 cage has been reported before.[2b] The increased flexibility of $[Pd_2\mathbf{1}_4]^{4+}$ compared to $[Pd_2\mathbf{2}_4]^{4+}$, the smaller size of $[Pd_2\mathbf{2}_4]^{4+}$, and the increased stability of the BF_4^- complex with $[Pd_2\mathbf{2}_4]^{4+}$ together rationalizes the stark contrast in binding properties observed for both complexes.

Summary and conclusion

In summary, ligands were synthesized that bear two dipyridyl donor groups linked by an isophthalamide (**1**) or a dipicolinamide moiety (**2**). Both ligands formed $[Pd_2(Ligand)_4][BF_4]_4$ complexes in CD_2Cl_2 containing 5% dmso-d_6. Cage $[Pd_2(\mathbf{1})_4][BF_4]_4$ was shown to bind to *n*-octyl glycosides **3–6** with affinities of about 250–500 M^{-1} in the order **3** > **5** > **4** = **6**, and to nitrate anions with a 1 : 1 affinity K_a = 1862 M^{-1}. In sharp contrast, cage $[Pd_2(\mathbf{2})_4][BF_4]_4$ did not appear to bind to glycosides and bound to nitrate with a 1 : 1 affinity of merely 159 M^{-1}. The difference in binding properties could be rationalized based on the reduced flexibility and size of the $[Pd_2(\mathbf{2})_4]^{2+}$ cage, and its stronger complexation to a BF_4^- anion. It is thus concluded that preorganization of the amides in **2** by intramolecular NH···N hydrogen bonding has an adverse effect on the binding properties of $[Pd_2(\mathbf{2})_4]^{2+}$ compared to its CH analogue $[Pd_2(\mathbf{1})_4]^{2+}$, at least for *n*-octyl glycosides **3–6** and nitrate.

Conflicts of interest

There are no conflicts to declare.

Acknowledgements

This research was financially supported by the Netherlands Organization for Scientific Research (NWO) with VIDI grant number 723.015.006.

References

1 (*a*) M. Han, D. M. Engelhard and G. H. Clever, *Chem. Soc. Rev.*, 2014, **43**, 1848–1860; (*b*) Z. Li, N. Kishi, K. Yoza, M. Akita and M. Yoshizawa, *Chem. – Eur. J.*, 2012, **18**, 8358–8365; (*c*) A. Schmidt, A. Casini and F. E. Kuhn, *Coord. Chem. Rev.*, 2014, **275**, 19–36; (*d*) L. Xu, Y. X. Wang and H. B. Yang, *Dalton Trans.*, 2015, **44**, 867–890; (*e*) G. H. Clever and P. Punt, *Acc. Chem. Res.*, 2017, **50**, 2233–2243; (*f*) D. Bardhan and D. K. Chand, *Chem. – Eur. J.*, 2019, **25**, 12241–12269;

 This journal is © The Royal Society of Chemistry 2021

Open Access Article. Published on 12 jlijs 2021. Downloaded on 24.02.2026 07:36:42.
This article is licensed under a Creative Commons Attribution-NonCommercial 3.0 Unported Licence.

(*g*) H. Y. Hou, K. Zhou, F. L. Jiang, Q. H. Chen and M. C. Hong, *Isr. J. Chem.*, 2019, **59**, 140–150.

2 (*a*) S. Freye, J. Hey, A. Torras-Galan, D. Stalke, R. Herbst-Irmer, M. John and G. H. Clever, *Angew. Chem., Int. Ed.*, 2012, **51**, 2191–2194; (*b*) D. P. August, G. S. Nichol and P. J. Lusby, *Angew. Chem., Int. Ed.*, 2016, **55**, 15022–15026.

3 (*a*) M. Yamashina, M. Akita, T. Hasegawa, S. Hayashi and M. Yoshizawa, *Sci. Adv.*, 2017, **3**, 6; (*b*) D. Yang, L. K. S. Krbek, L. Yu, T. K. Ronson, J. D. Thoburn, J. P. Carpenter, J. L. Greenfield, D. J. Howe, B. Wu and J. R. Nitschke, *Angew. Chem.*, 2021, **60**, 4485–4490; (*c*) X. Schaapkens, E. O. Bobylev, J. N. H. Reek and T. J. Mooibroek, *Org. Biomol. Chem.*, 2020, **18**, 4734–4738; (*d*) X. Schaapkens, J. H. Holdener, J. Tolboom, E. O. Bobylev, J. N. H. Reek and T. J. Mooibroek, *ChemPhysChem*, 2021, **22**(12), 1187–1192.

4 (*a*) N. Yue, Z. Q. Qin, M. C. Jennings, D. J. Eisler and R. J. Puddephatt, *Inorg. Chem. Commun.*, 2003, **6**, 1269–1271; (*b*) N. L. S. Yue, D. J. Eisler, M. C. Jennings and R. J. Puddephatt, *Inorg. Chem.*, 2004, **43**, 7671–7681; (*c*) N. L. S. Yue, M. C. Jennings and R. J. Puddephatt, *Inorg. Chim. Acta*, 2016, **445**, 37–45.

5 (*a*) A. J. Baer, B. D. Koivisto, A. P. Cote, N. J. Taylor, G. S. Hanan, H. Nierengarten and A. Van Dorsselaer, *Inorg. Chem.*, 2002, **41**, 4987–4989; (*b*) D. Tripathy, A. K. Pal, G. S. Hanan and D. K. Chand, *Dalton Trans.*, 2012, **41**, 11273–11275.

6 (*a*) T. J. Mooibroek, B. J. J. Timmer, X. Schaapkens and A. Kooijman, *Angew. Chem., Int. Ed.*, 2021, **60**(29), 16178–16183; (*b*) O. Beyer, B. Hesseler and U. Luning, *Synthesis*, 2015, 2485–2495.

7 T. Tateishi, S. Takahashi, A. Okazawa, V. Marti-Centelles, J. Z. Wang, T. Kojima, P. J. Lusby, H. Sato and S. Hiraoka, *J. Am. Chem. Soc.*, 2019, **141**, 19669–19676.

8 C. Frassineti, S. Ghelli, P. Gans, A. Sabatini, M. S. Moruzzi and A. Vacca, *Anal. Biochem.*, 1995, **231**, 374–382.

9 (*a*) B. J. J. Timmer and T. J. Mooibroek, *Chem. Commun.*, 2021, DOI: 10.1039/D1CC02663A; (*b*) D. K. Chand, K. Biradha and M. Fujita, *Chem. Commun.*, 2001, 1652–1653; (*c*) L. P. Zhou and Q. F. Sun, *Chem. Commun.*, 2015, **51**, 16767–16770; (*d*) R. Sekiya, M. Fukuda and R. Kuroda, *J. Am. Chem. Soc.*, 2012, **134**, 10987–10997; (*e*) J. Lee, S. Lim, D. Kim, O. S. Jung and Y. A. Lee, *Dalton Trans.*, 2020, **49**, 15002–15008; (*f*) U. Siriwardane and F. Fronczek, *CSD Communication*, 2017, CCDC deposition Nr. 1562063; (*g*) T. Y. Kim, N. T. Lucas and J. D. Crowley, *Supramol. Chem.*, 2015, **27**, 734–745; (*h*) J. E. M. Lewis and J. D. Crowley, *Supramol. Chem.*, 2014, **26**, 173–181; (*i*) E. Sone, M. Sato, K. Yamanishi, C. Kamio, H. Takemoto and M. Kondo, *Dalton Trans.*, 2016, **45**, 894–898; (*j*) S. Samantray, S. Krishnaswamy and D. K. Chand, *Nat. Commun.*, 2020, **11**, 11.

10 T. Velasco, G. Lecollinet, T. Ryan and A. P. Davis, *Org. Biomol. Chem.*, 2004, **2**, 645–647.